Hole spins in an InAs/GaAs quantum dot molecule subject to lateral electric fields

Xiangyu Ma, Garnett W. Bryant, and Matthew F. Doty

Hole Spins in an InAs/GaAs Quantum Dot Molecule subject to Lateral Electric Fields

Xiangyu Ma[1], Garnett W. Bryant[2], Matthew Doty[1,3]

[1]*Dept. of Physics and Astronomy, University of Delaware, Newark, DE 19716*
[2]*Quantum Measurement Division and Joint Quantum Institute, National Institute of Standards and Technology,*
100 Bureau Drive, Stop 8423, Gaithersburg, MD 20899-8423 and
[3]*Dept. of Materials Science and Engineering, University of Delaware, Newark, DE 19716*[*]

(Dated: May 3, 2016)

There has been tremendous progress in manipulating electron and hole spin states in quantum dots or quantum dot molecules (QDMs) with growth-direction (vertical) electric fields and optical excitations. However, the response of carriers in QDMs to an in-plane (lateral) electric field remains largely unexplored. We computationally explore spin-mixing interactions in the molecular states of single holes confined in vertically-stacked InAs/GaAs QDMs using atomistic tight-binding simulations. We systematically investigate QDMs with different geometric structure parameters and local piezoelectric fields. We observe both a relatively large Stark shift and a change in the Zeeman splitting as the magnitude of the lateral electric field increases. Most importantly, we observe that lateral electric fields induce hole spin mixing with a magnitude that increases with increasing lateral electric field over a moderate range. These results suggest that applied lateral electric fields could be used to fine-tune and manipulate, in situ, the energy levels and spin properties of single holes confined in QDMs.

I. INTRODUCTION

In recent years there has been tremendous progress in controlling spin projections and spin interactions in solid state systems that could provide the foundation for quantum information processing devices.[1] Solid-state materials that have been explored for this application include: silicon dopants,[2] nitrogen vacancy (NV) centers in diamond,[3] gate-defined quantum dots (QDs),[4] and optically-active self-assembled QDs.[5,6] Although initial efforts focused on electron spins, hole spins have recently attracted considerable attention due to the significant reduction in hyperfine interactions with nuclear spins, which are a primary source of dephasing and decoherence for qubits based on electron spins.[7–9] Continued progress toward the development of quantum device technologies based on hole spins requires a detailed understanding of the physical properties of hole spin states in candidate materials and the ways in which these properties can be manipulated by external stimuli.

In this paper we explore the spin properties of single holes confined in InAs/GaAs quantum dot molecules. The experimental system we model consists of two InAs QDs aligned along the growth direction and separated by a thin layer of GaAs, as depicted in Fig. 1a. Such a complex of multiple QDs is called a quantum dot molecule (QDM) because coherent interactions between two or more adjacent QDs lead to delocalized molecular-like wavefunctions with unique and tunable properties.[10–19] We focus specifically on a QDM in which the relative size of the two QDs and the electric field applied along the growth direction enables coherent tunneling of holes.[20] In the simplest picture, one can consider a QDM in which a hole with heavy-hole spin projection up is located in either the bottom $((\Uparrow, 0))$ or top $((0, \Uparrow))$ QD. When electric fields applied along the molecular stacking axis bring the discrete energy levels of the top and bottom QDs into resonance, coherent tunneling leads to the emergence of molecular states that can be described as the sum and difference of the basis states (e.g. $(\Uparrow, 0) \pm (0, \Uparrow)$). When a magnetic field B_z is applied along the growth axis (z), the spin degeneracy of the hole ground states in each QD is broken and a Zeeman splitting of each molecular branch is observed. Figure 1b shows the resulting four molecular states, with each state labelled at the right side of the figure by the atomic-like basis state that describes the state at an electric field where coherent interactions are negligible.

Due to the complex nature of the valence band, molecular states created by the coherent tunneling of holes can have surprising properties, including antisymmetric molecular ground states.[21] We focus here on the emergence of hole spin mixing, which is conceptually equivalent to a spin-flip coherent tunneling process that mixes states with opposite heavy-hole spin character (e.g. $(\Uparrow, 0) \pm (0, \Downarrow)$).[22] Such hole spin mixing manifests as an anticrossing between Zeeman-split molecular orbitals with opposite heavy-hole spin character, as indicated by the Δ_{sm} in Fig. 1c. This hole spin mixing interaction presents an opportunity to create wavelength-tunable qubit states compatible with all-optical information processing and scalable production of photonic information processing device architectures.[23] The hole spin mixing that has been observed to date is understood to arise from a lateral offset of the two QDs along the stacking axis (see bottom panel of Fig. 1a).[22] The symmetry breaking provided by the lateral offset allows light-hole components of the hole spinor to mediate a spin-orbit interaction that creates the hole spin mixing.[22,24–26] Larger offsets (Δx) create stronger spin mixing interactions that are advantageous for all-optical information processing schemes and

manifest as larger spin mixing anticrossings (Δ_{sm}). Although lateral offsets frequently occur in QDMs grown by molecular beam epitaxy, the typical offset distance is relatively small and cannot be controlled by growth techniques.[22]

We explore spin mixing interactions in the molecular states of single holes confined in InAs QDMs subject to two-dimensional electric fields that have components both parallel and perpendicular to the molecular stacking axis. Zhou, et al. recently presented a design for a device that can generate such fields around single QDMs.[27] Our objective in this paper is to understand the physical interactions that contribute to the emergence of hole spin mixing and to evaluate the possibility of using externally applied electric fields to reversibly control the magnitude of hole spin mixing interactions. We pursue this objective by computing the energies of QDM states under various electric and magnetic field conditions with a combination of tight binding atomistic calculations and matrix-based extrapolation of the atomistic results. We choose tight binding-based simulations over continuous methods such as $k \cdot p$ theory due to the advantages of tight binding in capturing the effects of atomistic symmetry, material interfaces, strain, and piezoelectricity[28] without the computational cost of the atomistic empirical pseudopotential methods. To understand the physical origin of observed phenomena, we systematically apply the methods to QDMs both with and without lateral offsets and compute results both with and without the inclusion of piezoelectric fields.
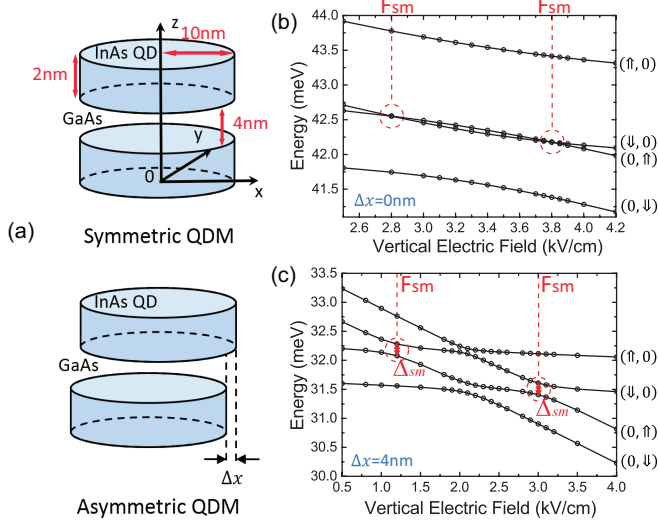

FIG. 1: (Color Online) (a) Disk shaped QDMs without (symmetric) and with (asymmetric) lateral offset. (b and c) The four lowest-energy hole states as a function of vertical (z-direction) electric field in a symmetric QDM for $B_z = 12$ T (b) and asymmetric QDM with $\Delta x = 4$ nm and $B_z = 6$ T (c).

II. METHODOLOGY

Figure 1a shows the two types of QDMs (symmetric and asymmetric) used in our calculation. Both types of QDMs consist of two disk-shaped InAs QDs that are 2 nm high and have a 10 nm radius. The QDs are vertically stacked along the z axis and are separated by a 4 nm thick GaAs barrier. The QDs of the symmetric QDM are perfectly aligned along the z axis while the asymmetric QDM has a top QD laterally offset by Δx. We compute the energy levels of these QDMs in the presence of electric and magnetic fields with an atomistic tight binding simulation that includes strain and spin-orbit interactions.

For the tight-binding calculations employed here, we use a $s3ps^*$ model.[29–32] In this model, the basis states for each atom include an s orbital, three p orbitals and an excited s^* orbital. Tight-binding parameters for InAs and GaAs that describe the on-site orbital energies and the coupling between nearest-neighbor atoms are adjusted empirically to reproduce the InAs and GasAs bulk band structure.[29] Spin-orbit effects are also included.[33,34] InAs/GaAs QDs are defined both by the band offset of the heterojunction and by the strain due to the lattice mismatch of the InAs and GaAs. The strain due to lattice mismatch is accounted for by use of the valence force field method to find the relaxed lattice configurations with the minimum strain energy.[30–32,35] The tight-binding parameters are rescaled using Harrison scaling laws to account for deviations of the local atomic lattice from the bulk configuration with bulk bond lengths and bond angles. Different electric and magnetic fields are used to manipulate the QD electronic structure. A static applied electric field is included in the tight-binding approach via a potential energy shift of the atomic orbital energies. A constant, static magnetic field is incorporated, in a gauge-invariant form, in the tight-binding approach via a Peierls transformation[36] that includes the magnetic vector potential via a phase shift of the tight-binding nearest-neighbor hopping parameters. The interaction with atomic orbital angular momentum and spin is also included with an additional Zeeman energy, $\mu_B(\vec{L}_{at} + 2\vec{S}) \cdot \vec{B}$ where $\vec{L}_{at}$ is the atomic orbital angular momentum and $\vec{S}$ is the spin. In piezoelectric materials, like III-V semiconductors such as InAs and GaAs, local strain produces local charge that is proportional to the strain. This local charge creates an additional local electric field and corresponding potential. We use the approach employed by Zielinski[37,38] to include the potential for the piezoelectric field as an additional shift of the on-site orbital energies.

The open circles in Figures 1b and c show the energies of the four lowest-energy hole states of the symmetric and asymmetric QDMs, relative to the lowest hole state in a single dot, as computed by our atomistic tight-binding method. These state energies are displayed as a function of the electric field applied along the growth direction in the presence of a constant 12 T (for the symmetric QDM) and 6 T (for the asymmetric QDM) magnetic field along

the growth direction. As shown in Fig. 1b for the symmetric QDM, the degeneracy of the hole states with opposite spin projections is broken by the applied magnetic field and four states are observed. Away from the crossing these states can be assigned to the heavy-hole spin states $(\Uparrow, 0)$, $(\Downarrow, 0)$, $(0, \Uparrow)$, and $(0, \Downarrow)$, with the hole located in the bottom (left) or top (right) QD, respectively. For the asymmetric QDM, hole spin mixing manifests as an anticrossing between two states that have opposite heavy-hole spin projection far away from the anticrossings. Molecular states that are complex mixtures of these QD states are formed near and between the anticrossings for the asymmetric QDM in Fig. 1c. For the asymmetric QDM, whose state energies are shown in Fig. 1c, two such anticrossings are observed, at 1.1 kV/cm and 3.2 kV/cm. We will use F_{sm} to represent the vertical electric fields at which hole spin mixing can occur and the anticrossing gap Δ_{sm} to characterize the strength of the hole spin mixing interaction. In Fig. 1b no anticrossing is observed at the F_{sm} points because the QDM is symmetric and the electric field has components only along the z axis.

We note that the magnetic field values for our computations are chosen so that hole spin mixing effects can be quantitatively extracted from the computed energy levels of the states as a function of both lateral and vertical electric field. Specifically, we choose magnetic fields at which hole states with opposite spins in the two QDs come into resonance. The magnetic field required to create this degeneracy depends on both the strength of coherent tunneling and the hole g-factor, as shown in several previous experiments.[13,15,20,22] This is the reason that different magnetic fields (6 T vs 12 T) are used in Fig. 1b and c for symmetric and antisymmetric QDMs, respectively. A further consequence of this variation is a change in the electric fields of maximum spin mixing, F_{sm} in Fig. 1b and c. As a result of this change, different x scales are used in Figs. 1b and c. The difference in x scales creates the illusion of a different electric field dependence for the indirect optical transitions between these two cases, but the dependence is, in fact, the same.

Although the atomistic tight binding method provides a precise computation of both the state energies and the corresponding state wavefunctions, it is computationally intensive. To reduce the number of full tight-binding calculations needed, we first do a tight-binding calculation at a chosen electric field $\vec{F}_0$ to define a basis of exact eigenstates for this field. Using this basis, we then calculate eigenstates for other fields by diagonalizing the following matrix Hamiltonian:

$$H' = \begin{bmatrix} E_1^{(0)} + V_{11} & V_{12} & \dots & V_{1n} \\ V_{21} & E_2^{(0)} + V_{22} & \dots & V_{2n} \\ \vdots & \vdots & \ddots & \vdots \\ V_{n1} & V_{n2} & \dots & E_n^{(0)} + V_{nn} \end{bmatrix} \quad (1)$$

In the following, we refer to this as the matrix Hamilto-

nian method to distinguish it from our full tight-binding calculations.

The basis states for this matrix are the first n hole states, with energies $E_n^{(0)}$ as computed by the atomistic method. The wavefunction that describes each state (ϕ_i) consists of amplitudes for every electron orbital (s, p and s*) at each atomic site. The external potential $V = (\vec{F} - \vec{F}_0) \cdot \vec{r}$ is based on the electric field ($\vec{F}$) and the position of each atom ($\vec{r}$). The interaction terms (V_{ij}) are constructed from the integration of two wavefunctions over the electric potential, $V_{ij} = \langle \phi_i | V | \phi_j \rangle$, which is performed as a sum over every atomic site. The eigenvalues of the matrix Hamiltonian provide the energies of the hole states under the external electric field.

For computational efficiency we want to include in our matrix Hamiltonian calculations the minimum number of basis states required to generate a sufficiently precise result. We therefore test the matrix Hamiltonian calculations by computing the matrix Hamiltonian results as a function of the number of basis states included and comparing these results to atomistic simulations. We use basis states generated by the tight-binding method under a constant electric field along the z axis. We then use our matrix Hamiltonian (Eq. 1) to compute the energy levels under an electric field applied along the x and z axis. We compare the matrix Hamiltonian results to the full tight-binding calculations under the same electric field conditions (e.g. with electric fields along both x and z). We performed this test for multiple field configurations and found that our matrix Hamiltonian results converge to a precision of at least 97 %, relative to the full tight-binding results, so long as we include at least the 16 lowest-energy hole states (i.e. the 16 states closest to the valence band edge). Throughout the remainder of this paper, results computed by the matrix Hamiltonian method will be indicated by lines and results computed by full tight-binding calculations will be indicated by open circles. The good agreement between tight-binding and matrix Hamiltonian results can be seen in each figure.

We now present a systematic analysis of hole spin mixing in QDMs under four different conditions: both with and without lateral offsets and both with and without the inclusion of piezoelectric fields. All calculations are performed under a constant magnetic field applied along the z axis. Initial basis states are generated by full tight-binding calculations and the matrix Hamiltonian method is used to explore variations in the electric field. Full tight-binding calculations for certain electric fields are performed to validate the matrix Hamiltonian results. In each case we first consider the energy levels and Zeeman splittings of the hole states under a constant 'vertical' electric field (along the z axis) as a function of the 'lateral' electric field (along the x axis). Second, we explore the magnitude of hole spin-mixing induced by the lateral electric field. Third, we consider the hole wavefunctions to probe the impact of the lateral electric fields on the spatial distribution of the hole. In all of these cases the
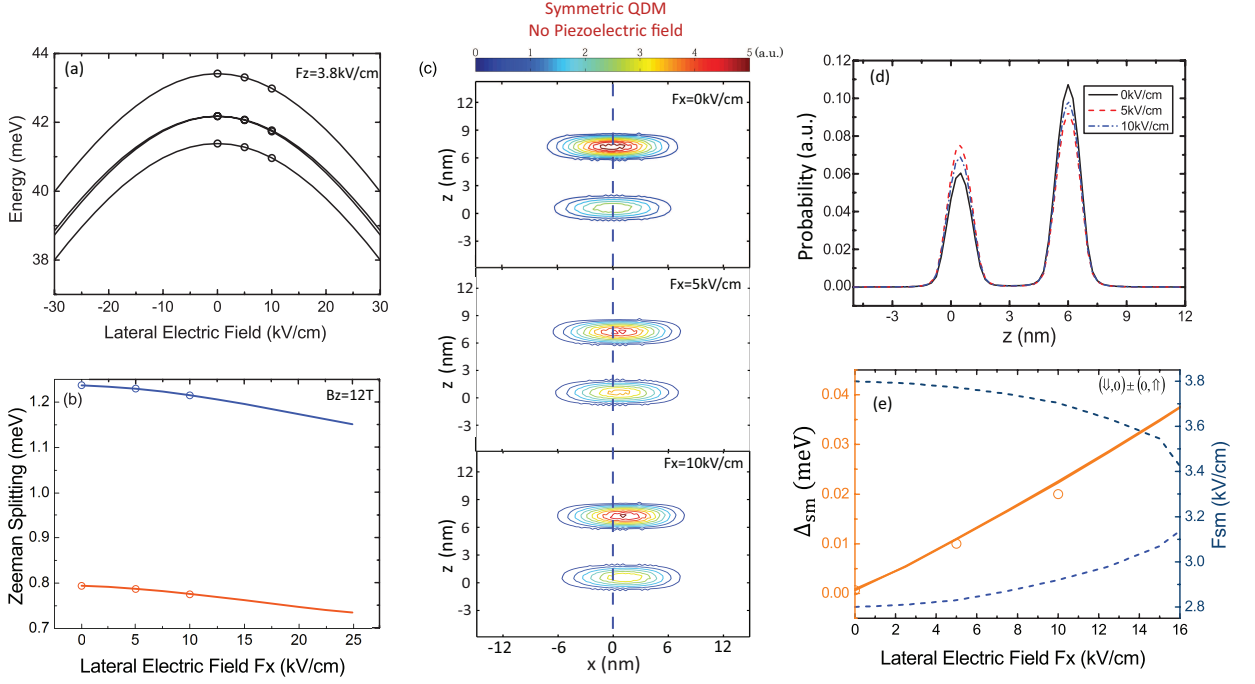
FIG. 2: (Color Online)Effect of a lateral (x-direction) electric field on a symmetric QDM under a constant 12 T magnetic field in the absence of piezoelectric fields. (a and b). Energy (a) and Zeeman splitting (b) of the four lowest-energy hole states as a function of lateral electric field when $F_z = 3.8$ kV/cm. (c and d) Spatial distribution of a hole wavefunction in $y = 0$ plane (c) and along z axis (d) with different lateral electric fields as derived from the full tight-binding results. (e) Spin mixing anticrossing splitting (Δ_{sm}) and spin mixing resonance vertical electric field (F_{sm}) as a function of lateral electric field.

lateral electric field is constant along the z axis. In the final section we explore hole spin-mixing in response to lateral electric fields that have a gradient along the z axis, so that a different lateral field acts on each dot and further breaks the symmetry between dots.

III. RESULTS

A. Symmetric QDM without piezoelectric field

To systematically analyze the effects of lateral electric fields on QDM spin states, we first consider a symmetric QDM in the absence of piezoelectric fields. Figure 2a plots the energies of the four lowest-energy hole states as a function of lateral electric field applied along the x axis. For clarity, we present the hole energy relative to the lowest hole energy in a single dot instead of the absolute hole energy value. A constant magnetic field $B_z = 12$ T and vertical electric field $F_z = 3.8$ kV/cm are applied. This value of F_z brings states with opposite heavy-hole spin character into resonance. The results computed with our matrix Hamiltonian method are based on the basis states computed with the full tight-binding approach for zero lateral electric field. Both tight-binding and matrix Hamiltonian results indicate that the energy of the hole states decreases with increasing lateral electric field. The state energy decreases by about 3.5 meV when a

30 kV/cm lateral electric field is applied. The nearly parabolic decrease in energy largely arises from the Stark shift by the lateral field. However, the Stark shift when electric fields are applied along the lateral direction tunes the state energy over a much larger range than the Stark shift for an electric field applied along the growth direction. This larger tuning range for lateral electric fields is due to the extended distribution of the hole wavefunction in the lateral direction. Thus, lateral electric fields may provide a method for fine-tuning the optical transition energies of QDs or QDMs for use in device applications.

Figure 2b plots the Zeeman splitting of the hole states as a function of applied lateral electric field, with a constant magnetic field $B_z = 12$ T and vertical electric field $F_{sm} = 3.8$ kV/cm. Previous work on InAs QDMs has shown that the Zeeman splitting between spin projections can be a function of applied vertical electric field due to the changing spatial distribution of electron or hole wavefunctions.[13,15,39–42] In our case, the changing Zeeman splitting originates, at least in part, from the changing spatial extent of the hole wavefunctions induced by the applied lateral electric field. This dependence of the hole wavefunction distribution on lateral field is displayed in Figure 2c. Figure 2c shows the spatial distribution of the third-lowest hole state wavefunction in the $y = 0$ spatial plane computed directly from tight-binding results for three different lateral electric fields. We see that the charge density of the heavy hole is some-

what larger in the top dot than the bottom dot. This is because the result is computed at the applied vertical field for maximum hole spin mixing, which is a vertical electric field slightly detuned from the resonant field for spin-conserving tunneling at which the charge density in the two QDs would be equal. The displacement of the wavefunctions in both QDs relative to the blue dashed line at $x = 0$ can be seen to increase with increasing lateral electric field. However, the relative contributions of changing atomic spin polarization and orbital angular momentum to this changing Zeeman splitting are not presently understood.

The vertical electric field controls the energy offset between hole states in the two QDs and thus the localization/delocalization of the hole state along the growth axis. The Zeeman splitting reduction should also result in changes of the hole distribution along the z-axis because the shift in Zeeman splitting changes the resonance between the hole states in the separate QDs. Fig. 2d shows that the hole distribution along the growth axis changes non-monotonically with increasing lateral electric field. The hole state is more delocalized with a non-zero lateral electric field (5 kV/cm) than for zero lateral electric field. However, the hole state becomes more localized as the lateral electric field increases further (10 kV/cm). We believe that this non-monotonic behavior originates in the competition between multiple effects, including Zeeman splitting reduction and hole spin mixing.

To directly analyze the impact of lateral electric fields on hole spin mixing, Fig. 2e plots the hole spin mixing magnitude (Δ_{sm}) and spin mixing resonance vertical electric field (F_{sm}) as a function of lateral electric field. We observe a nearly linear increase of Δ_{sm} with the increase of lateral electric field in both the full tight-binding and matrix Hamiltonian calculations. The non-zero value for Δ_{sm} for non-zero lateral electric fields demonstrates that lateral electric fields could be used to controllably turn on the hole spin mixing effect, although the strength of the hole spin mixing interaction is relatively weak. In principle larger lateral electric fields could be used to increase the strength of the interaction. However, the Zeeman splitting reduction displayed in Fig. 2b shifts the energies of the involved states and causes the two spin mixing anticrossing points (F_{sm}) to approach one another, as displayed by the right axis in Fig. 2e. As a result of this energy shift, the states ($\Downarrow, 0$) and ($0, \Uparrow$) no longer intersect and no spin mixing anticrossing can be resolved for lateral electric fields more than 20 kV/cm. Although there are likely complex spin mixing interactions present for larger lateral electric fields, we focus here on the spin mixing interactions that can be quantified by the magnitude of spin mixing anticrossings.

To summarize this section, lateral electric fields can induce a Stark shift with a larger energy tuning than that induced by growth direction electric fields. Lateral electric fields further modulate the energy level of holes in symmetric QDMs by both shifting and shrinking the hole wavefunction in the lateral direction. As a consequence of these wavefunction changes, increasing lateral electric fields cause the hole to become less sensitive to growth direction magnetic fields, causing a reduction of the Zeeman splitting. Finally, lateral electric fields induce hole spin mixing with a magnitude that increases with increasing lateral electric field over a moderate range. These results demonstrate that applied lateral electric fields provide an opportunity to fine-tune, in situ, the energy levels and spin properties of holes in QDMs.

B. 1 nm shifted QDM without piezoelectric field

Lateral offsets in QDMs are commonly observed experimentally, with an average lateral offset of about 1.8 nm.[22] The magnitude of this offset cannot be controlled and can only be directly measured with destructive techniques. From a QDM device engineering point of view, however, QDMs with small lateral offsets should be considered as they will commonly occur. From a physics point of view it is important to understand what hole spin properties change as a result of nonzero lateral offset. We therefore explore the hole states of an asymmetric QDM with $\Delta x = 1$ nm as a function of applied lateral electric field. In this section we continue to exclude piezoelectric fields. Unlike the case of symmetric QDMs, in which the direction of the lateral electric field is not important, in asymmetric QDMs the direction of the lateral electric field relative to the shift direction plays an important role. We therefore consider two cases: lateral electric field along the shift direction (F_x) and lateral electric field perpendicular to the shift direction (F_y). We use basis states obtained by a full zero-lateral-field tight-binding calculation and then extrapolate with our matrix Hamiltonian method to consider the effect of lateral electric fields.

When we apply a lateral electric field (F_y) that is perpendicular to the lateral offset direction (x), we find that the hole states respond in a manner similar to when a lateral electric field is applied to non-shifted QDMs, as described in Section III A. Figure 3(a) shows the energies of the four lowest-energy hole states as a function of F_y under a constant vertical electric field $F_z = 3$ kV/cm and magnetic field $B = 12$ T. Lateral electric fields in both $\pm$ directions will cause a Stark shift in the hole state energies with a magnitude similar to that in symmetric QDMs. Figure 3(b) shows the magnitude of the two hole spin-mixing anticrossings, Δ_{sm}, and the two resonance vertical electric fields, F_{sm}, as a function of F_y. Due to the symmetry breaking of the QDM, a hole spin-mixing anticrossing $\Delta_{sm} = 0.18$ meV is formed when $F_y = 0$. A lateral electric field along y modulates the magnitude of the hole spin mixing interaction in a direction-dependent manner. Both the offset and the lateral electric field contribute to the symmetry breaking in the QDM. However, for lateral fields along $+y$, the (110) component of the lateral field and the QDM shift are parallel. For lateral electric fields along $-y$, the two components are an-
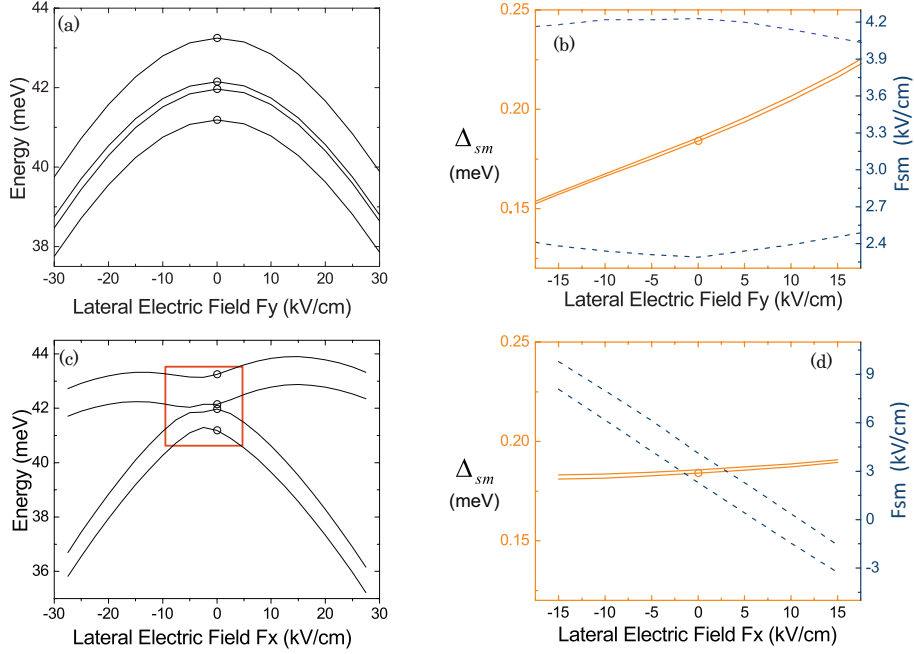
FIG. 3: (Color Online) Effect of lateral electric field on an asymmetric QDM for $B = 12$ T, in the absence of piezoelectric field. (a) Energy level of the lowest four hole states for $B = 12$ T and $F_z = 3$ kV/cm, as a function of lateral electric field (F_y) perpendicular to the QDM offset direction (x). (b) Spin mixing splitting amplitude Δ_{sm} (yellow solid line) and spin mixing resonance vertical electric field F_{sm} (blue dashed line) as a function of F_y. (c) Energy levels of hole states as a function of lateral electric field along the QDM's offset direction, F_x. (d) Δ_{sm} and F_{sm} as a function of lateral electric field F_x.

tiparallel. A similar effect has been reported in QDMs subject to external strains, which provides an alternative path toward controllable hole spin mixing in QDMs.[43] We observe a Zeeman splitting reduction in this asymmetric QDM with similar magnitude to that observed for a symmetric QDM. In summary, lateral electric fields orthogonal to the QD shift direction modify hole states in a manner similar to the effect on perfectly aligned QDs, with the exception that the field direction determines whether the hole spin mixing magnitude increases or decreases.

Lateral electric fields along the QD shift direction (x) impact the hole state energies in a manner that changes the molecular resonance field F_{sm}. Figure 3(c) shows the energies of the four lowest-energy hole states under a constant vertical electric field as a function of lateral electric field along x (i.e. F_x). The dependence on F_x highlighted by the red square in Figure 3(c) appears qualitatively similar to the energy levels as a function of vertical electric field shown in Fig. 1c. However, the vertical field needed to induce the resonance shifts significantly when a lateral field is applied along x. These shifts in the anticrossing energies originate in changes to the molecular wavefunctions. We calculate and observe that the x direction electric field shifts the hole wavefunctions along x in a manner similar to the shifts observed in symmetric QDMs and presented in Figure 2(c) and (d). We also confirm that the wavefunction overlap in the vertical direction for these asymmetric QDMs is perturbed by the

lateral shifts induced by the x direction electric field. As a result, the vertical electric field required to create fully delocalized molecular states changes.

For the calculations displayed in Fig. 3(c), which are computed at a fixed vertical electrical field, the shift in state energies that arises when the electric field is applied along x effectively results in a detuning from the vertical electric field that creates the molecular resonance. We also analyze the hole spin-mixing anticrossing magnitude Δ_{sm} as a function of an electric field along x. As indicated in Figure 3(d), the magnitude of the spin mixing anticrossing stays nearly constant as a function of F_x. This is not surprising because the lateral electric field shifts the hole wavefunctions in each QD similarly in the x direction, thus the electric field applied along the shift axis does not introduce any significant change to the broken symmetry of the QDM.

In summary, lateral electric fields perpendicular to the QDM shift direction introduce energy shifts similar to those observed when lateral electric fields are applied to a symmetric QDM. Moreover, the magnitude of hole spin mixing can be increased or decreased depending on the direction of the applied field. Lateral electric fields parallel to the shift direction change the resonance field needed to form the molecular hole state. However, electric fields along the shift axis have little impact on the symmetry breaking or hole spin mixing.
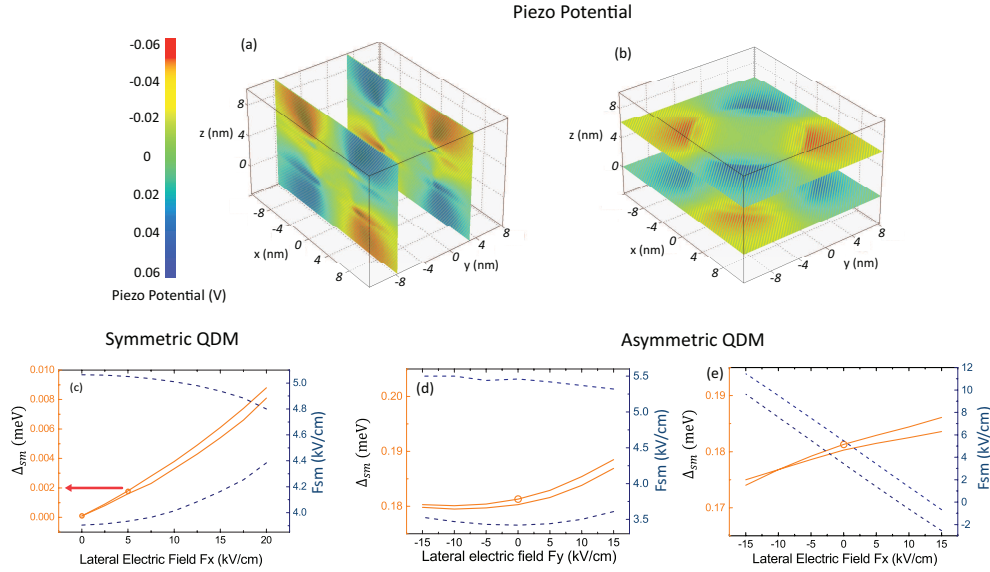
FIG. 4: (Color Online) Effect of lateral electric field on a symmetric QDM under 12 T constant magnetic field with the piezoelectric field. Planes of the piezo potential at the edge of the QDs (a) and the middle of the QDs (b). (c),(d),(e) Spin mixing splitting amplitude Δ_{sm} (orange) and spin mixing resonance vertical electric field F_{sm} (blue) as a function of lateral electric field in different directions, ((c) Symmetric QDM, (d),(e) asymmetric QDM))

C. QDM with piezoelectric field

In the previous sections we explored the effect of lateral electric field on symmetric and asymmetric QDMs without including the piezoelectric field. However, strain-induced piezoelectric fields can make an important contribution to the local electric field of the QDM. We include piezoelectric effects in our tight-binding calculations as described in the methodology section. We repeat the process of calculating the energy levels of symmetric and asymmetric QDMs under applied electric fields with piezoelectric fields included. We analyze the results to understand the physical consequences of the piezoelectric fields and their interplay with QDM symmetry and applied lateral electric fields.

Figure 4(a) and (b) display two different 2D cross-sectional planes of the piezoelectric potential of a symmetric QDM. The vertical planes in Figure 4(a) lie at the outer edges of the two QDs and the horizontal planes in Figure 4(b) lie at the middle of each QD. These figures show that piezoelectric potential dipoles are formed at the corner of each quantum dot, but with a 90° rotation of the dipole orientation between the two dots. The symmetry of piezoelectric potentials has been found to depend on a variety of parameters.[25,44,45] The rotated symmetry we find occurs when QDs are close together and act as a strongly coupled entity.[44] Under a constant lateral electric field, we observe Stark shifts and Zeeman splitting reduction similar to QDMs without piezoelectric fields with only small shifts in the resonant electric fields at which molecular states are formed. However, piezoelectric fields substantially change the magnitude and tuning range of hole spin mixing, as we now discuss.

Figure 4(c) plots the Δ_{sm} and F_{sm} for the two hole spin mixing anticrossings of a symmetric QDM as a function of a lateral electric field along x. Because the QDM is symmetric, piezoelectric fields by themselves are not sufficient to induce hole spin mixing and two crossings occur as a function of applied vertical electric field. In other words, $\Delta_{sm} = 0$ for $F_x = 0$. Anticrossings at both F_{sm} emerge when a non-zero lateral electric field is applied ($F_x > 0$). Zeeman splitting effects (not shown) cause the two F_{sm} to converge with increasing lateral electric field as described above. Although the emergence of non-zero Δ_{sm} as a function of F_x is qualitatively similar to what is observed in the absence of piezoelectric fields, the magnitude of Δ_{sm} is substantially reduced. As shown in Fig. 4(c), Δ_{sm} at $F_x = 15$ kV/cm is about 6 μeV, much smaller than the 35 μeV anticrossing observed in the absence of piezoelectric fields (Fig. 2).

We next explore the consequences of including piezoelectric fields in the simulations of asymmetric QDMs with $\Delta x = 1$ nm. Following the analysis described above, we consider lateral electric fields perpendicular to (F_y) and parallel to (F_x) the lateral offset direction (x). The results are presented in Figure 4(d) and (e), respectively. In both cases, the Δ_{sm} value remains nearly constant as a function of lateral electric field. For electric fields parallel to the shift axis (Figure 4(e)), this result is similar to what is observed without the inclusion of piezoelectric fields (Fig. 3(d)). We therefore conclude that the inclusion of piezoelectric fields does not significantly alter the physics of hole spin mixing for electric fields along the shift axis. For electric fields perpendicular to the shift axis (Figure 4(d)), the change in Δ_{sm} is about 7 times smaller than that observed when piezoelectric fields are

not included (Fig. 3(b)). This suggests that the symmetry breaking induced by the applied lateral electric field is largely compensated by the local piezoelectric field.

In summary, the emergence and evolution of hole spin mixing is qualitatively similar for QDMs studied with and without the inclusion of piezoelectric fields. However, the magnitude of hole spin mixing interactions (Δ_{sm}) is reduced when piezolectric fields are included. Piezoelectric fields are inherent to the InAs/GaAs QDM system, and thus intentional generation of strong spin mixing interactions using constant lateral electric fields will be challenging. A physical interpretation of the relatively weak tuning with constant electric fields is that hole wavefunctions in the two QDs are displaced by similar amounts when the same electric field is applied to each QD. As a result, constant electric fields do not substantially alter the symmetry of the electronic states of the QDM. This suggests that a gradient in the lateral field, with different lateral fields applied to each dot, may enhance the symmetry breaking. We next explore the consequences of lateral electric field profiles that have a gradient with different lateral field magnitudes at the locations of the two QDs that comprise the QDM.

D. Lateral electric fields with a gradient

To investigate the effects of an electric field with a gradient, we compute the energies of the hole states in an asymmetric QDM when the applied lateral electric field along y (F_y) has a gradient along the growth direction. We choose the lateral electric field profile so that the direction of the field is reversed in different dots, and then compute energy states for a gradient $G_{yz} = \frac{\partial F_y}{\partial z} = \frac{\partial F_z}{\partial y}$. We consider G_{yz} values ranging from 0 to 0.002 (mV/Å)/Å. For this gradient, there is a G_{yz} mV/Å change in the amplitude of F_y for every Å step along the z axis. In compliance with Maxwell's equations, the same gradient occurs in the vertical electric field (F_z) as a function of lateral position (y). The electric field along the y axis (F_y) as a function of y and z position coordinates is $F_y = 5$ kV/cm $+G_{yz}z$.

The results presented here are computed with the matrix Hamiltonian approach using basis states obtained with atomistic tight binding for the asymmetric QDM without a lateral electric field. Figure 5(a) shows the electric potential in the plane of the two QDs when $G = 0.002$ (mV/Å)/Å. The red arrows indicate the direction and relative magnitude of F_y. The oppositely oriented electric fields in the planes of the two QDs will cause the hole wavefunctions to shift in opposite directions, breaking the QDM symmetry in a manner similar to the lateral shift that occurs in asymmetric QDMs. This range of electric field gradient around single QDMs can be easily achived by the device designed by Zhou, et al.[27]

Figure 5(c) shows the hole spin mixing Δ_{sm} and resonance electric field F_{sm} as a function of the gradient magnitude G_{yz}. The magnitude of hole spin mixing Δ_{sm}
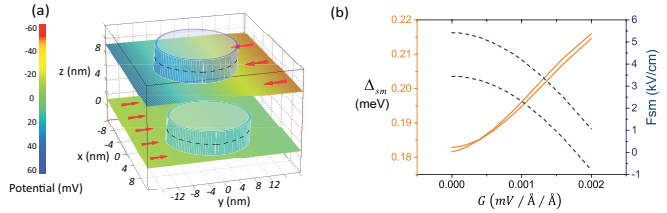

FIG. 5: (Color Online) Effect of lateral electric field with a gradient in the growth direction on asymmetric QDMs with piezoelectric fields included. (a) Electric potential for gradient $G_{yz} = 0.002$ (mV/Å)/Å . (b) Δ_{sm} (orange) and F_{sm} (blue) as a function of lateral electric field gradient G.

increases with increasing gradient magnitude. The range of Δ_{sm} values accessible for this range of G_{yz} is still limited, possibly because of the strong piezoelectric fields, and thus larger field gradients would likely be desirable for device applications. F_{sm} shifts with G_{yz} due to the changes in both F_y and F_z. Unlike the case with constant lateral electric field, we do not observe a Zeeman splitting reduction as a function of increasing gradient magnitude. As a result, the spacing between the two F_{sm} is nearly independent of G_{yz}.

IV. CONCLUSION

We use tight-binding atomistic simulations and a finite-basis matrix Hamiltonian extrapolation method to explore the effects of lateral electric fields on holes confined in vertically-stacked InAs/GaAs QDMs. We systematically considered the effects of QDM asymmetry, piezoelectric fields and electric field gradients. We find that constant lateral electric fields can be used to change the hole state energy and can also be used to reduce the Zeeman splitting of hole spin states. These results suggest that lateral electric fields could be used to tune the spin splitting or optical emission energies of QDMs for photonic device applications. We also find that constant lateral electric fields can be used to modulate the magnitude of hole spin mixing in both symmetric and asymmetric QDMs. Although the magnitude of the hole spin mixing interaction increases with applied field, the simultaneous reduction in Zeeman splitting restricts the range of hole spin mixing values that can be achieved. Lateral electric fields with a gradient in the growth direction enhance the tuning of the hole spin mixing interaction without reducing the Zeeman splitting. Our analysis shows that piezoelectric fields in the QDM reduce the sensitivity of the hole spin mixing magnitude to applied lateral electric fields, suggesting that different structures with different piezoelectric field environments could be explored to overcome this limitation. Future exploration of these effects in QDMs with a range of sizes, barrier thicknesses, and barrier compositions will

provide important information on the design of quantum dot molecules for quantum device applications.

V. ACKNOWLEDGEMENT

* Electronic address: doty@udel.edu

[1] D. D. Awschalom, L. C. Bassett, A. S. Dzurak, E. L. Hu, and J. R. Petta, Science **339**, 1174 (2013).

[2] J. J. Morton, D. R. McCamey, M. A. Eriksson, and S. A. Lyon, Nature **479**, 345 (2011).

[3] M. G. Dutt, L. Childress, L. Jiang, E. Togan, J. Maze, F. Jelezko, A. Zibrov, P. Hemmer, and M. Lukin, Science **316**, 1312 (2007).

[4] J. Petta, A. C. Johnson, J. Taylor, E. Laird, A. Yacoby, M. D. Lukin, C. Marcus, M. Hanson, and A. Gossard, Science **309**, 2180 (2005).

[5] X. Li, Y. Wu, D. Steel, D. Gammon, T. Stievater, D. Katzer, D. Park, C. Piermarocchi, and L. Sham, Science **301**, 809 (2003).

[6] A. Srivastava, M. Sidler, A. V. Allain, D. S. Lembke, A. Kis, and A. ImamoÄŸlu, Nature Nanotechnology **10**, 491 (2015).

[7] D. Brunner, B. D. Gerardot, P. A. Dalgarno, G. Wüst, K. Karrai, N. G. Stoltz, P. M. Petroff, and R. J. Warburton, Science **325**, 70 (2009).

[8] C. Testelin, F. Bernardot, B. Eble, and M. Chamarro, Physical Review B **79**, 195440 (2009).

[9] P. Fallahi, S. T. Yılmaz, and A. Imamoğlu, Physical Review Letters **105**, 257402 (2010).

[10] M. Bayer, P. Hawrylak, K. Hinzer, S. Fafard, M. Korkusinski, Z. Wasilewski, O. Stern, and A. Forchel, Science **291**, 451 (2001).

[11] H. J. Krenner, M. Sabathil, E. C. Clark, A. Kress, D. Schuh, M. Bichler, G. Abstreiter, and J.J. Finley, Physical Review Letters **94**, 057402 (2005).

[12] E. A. Stinaff, M. Scheibner, A. S. Bracker, I. V. Ponomarev, V. L. Korenev, M. E. Ware, M. F. Doty, T. L. Reinecke, and D. Gammon, Science **311**, 636 (2006).

[13] M. F. Doty, M. Scheibner, I. V. Ponomarev, E. A. Stinaff, A. S. Bracker, V. L. Korenev, T. L. Reinecke, and D. Gammon, Physical Review Letters **97**, 197202 (2006).

[14] M. F. Doty, M. Scheibner, A. S. Bracker, I. V. Ponomarev, T. L. Reinecke, and D. Gammon, Physical Review B **78**, 115316 (2008).

[15] W. Liu, S. Sanwlani, R. Hazbun, J. Kolodzey, A. S. Bracker, D. Gammon, and M. F. Doty, Physical Review B **84**, 121304 (2011).

[16] W. Liu, A. S. Bracker, D. Gammon, and M. F. Doty, Physical Review B **87**, 195308 (2013).

[17] X. Zhou, S. Sanwlani, W. Liu, J. H. Lee, Z. M. Wang, G. Salamo, and M. F. Doty, Physical Review B **84**, 205411 (2011).

[18] X. R. Zhou, J. H. Lee, G. J. Salamo, M. Royo, J. I. Climente, and M. F. Doty, Physical Review B **87**, 125309 (2013).

[19] X. Zhou, M. Royo, W. Liu, J. H. Lee, G. J. Salamo, J. I. Climente, and M. F. Doty, Physical Review B **91**, 205427 (2015).

[20] A. Bracker, M. Scheibner, M. Doty, E. Stinaff, I. Ponomarev, J. Kim, L. Whitman, T. Reinecke, and D. Gammon, Applied Physics Letters **89**, 233110 (2006).

[21] M. F. Doty, J. I. Climente, M. Korkusinski, M. Scheibner, A.S. Bracker, P. Hawrylak, and D. Gammon, Physical Review Letters **102**, 047401 (2009).

[22] M. F. Doty, J.I. Climente, A. Greilich, M. Yakes, A. S. Bracker, and D. Gammon, Physical Review B **81**, 035308 (2010).

[23] S. E. Economou, J. I. Climente, A. Badolato, A. S. Bracker, D. Gammon, and M. F. Doty, Physical Review B **86**, 085319 (2012).

[24] J. I. Climente, M. Korkusinski, G. Goldoni, and P. Hawrylak, Physical Review B **78**, 115323 (2008).

[25] F. Rajadell, J. Climente, and J. Planelles, Applied Physics Letters **103**, 132105 (2013).

[26] J. Planelles, F. Rajadell, and J. I. Climente, arXiv preprint arXiv:1505.06009 (2015).

[27] X. Zhou and M. Doty, Journal of Applied Physics **116**, 163101 (2014).

[28] M. Zieliński, Physical Review B **86**, 115424 (2012).

[29] P. Vogl, H. D. Hjalmarson, and J. D. Dow, Journal of the Physics and Chemistry of Solids **44**, 365 (1983).

[30] G. W. Bryant, M. Zieliński, N. Malkova, J. Sims, W. Jaskólski, and J. Aizpurua, Physical Review Letters **105**, 067404 (2010).

[31] G. W. Bryant, M. Zieliński, N. Malkova, J. Sims, W. Jaskólski, and J. Aizpurua, Physical Review B **84**, 235412 (2011).

[32] G. W. Bryant, N. Malkova, and J. Sims, Physical Review B **88**, 161301 (2013).

[33] D. J. Chadi, Physical Review B **16**, 790 (1977).

[34] K. C. Hass, H. Ehrenreich, B. Velicky, Physical Review B **27**, 1088 (1983).

[35] C. Pryor, J. Kim, L. W. Wang, A. J. Williamson, and A. Zunger, Journal of Applied Physics **83**, 2548 (1998).

[36] M. Graf and P. Vogl, Physical Review B **51**, 4940 (1995).

[37] W. Jaskolski, M. Zielinski, G. W. Bryant, and J. Aizpurua, Physical Review B **74**, 195339 (2006).

[38] T. Saito and Y. Arakawa, Physica E (Amsterdam) **15**, 169 (2002).

[39] W. Sheng, Applied Physics Letters **95**, 113103 (2009).

[40] W. Sheng, Applied Physics Letters **96**, 133102 (2010).

[41] J. van Bree, A. Y. Silov, P. M. Koenraad, and M. E. Flatte, Physical Review Letters **112**, 187201 (2014).

[42] J. van Bree, A. Y. Silov, P. M. Koenraad, and M. E. Flatte, Physical Review B **90**, 165306 (2014).

[43] E. Zallo, R. Trotta, V. Křápek, Y. H. Huo, P. Atkinson, F. Ding, T. Šikola, A. Rastelli, and O. G. Schmidt, Physi-

cal Review B **89**, 241303 (2014).

[44] T. Andlauer and P. Vogl, Physical Review B **79**, 045307 (2009).

[45] K. Gawarecki, P. Machnikowski, and T. Kuhn, Physical Review B **90**, 085437 (2014).